

# Single-Cysteine Substitution Mutants at Amino Acid Positions 306–321 in Rhodopsin, the Sequence between the Cytoplasmic End of Helix VII and the Palmitoylation Sites: Sulfhydryl Reactivity and Transducin Activation Reveal a Tertiary Structure<sup>†,‡</sup>

Kewen Cai,<sup>§</sup> Judith Klein-Seetharaman,<sup>§</sup> David Farrens,<sup>§,||</sup> Cheng Zhang,<sup>§,⊥</sup> Christian Altenbach,<sup>#</sup> Wayne L. Hubbell,<sup>#</sup> and H. Gobind Khorana<sup>\*,§</sup>

Department of Biology and Chemistry, Massachusetts Institute of Technology, Cambridge, Massachusetts 02139, and Jules Stein Eye Institute and Department of Chemistry and Biochemistry, University of California, Los Angeles, CA 90095-7008

Received January 4, 1999; Revised Manuscript Received April 8, 1999

**ABSTRACT:** As sensors for structure at the cytoplasmic face of rhodopsin, single-cysteine substitution mutants have been previously studied in the regions connecting helices III and IV and helices V and VI. In this paper we report on single-cysteine substitution mutants at amino acid positions 306–321, comprising the cytoplasmic sequence between helix VII and the palmitoylation sites in rhodopsin. The cysteine opsin mutants were expressed in COS-1 cells and on treatment with 11-*cis*-retinal all formed the characteristic rhodopsin chromophore. Cysteines at positions 306–316 and 319 reacted in the dark with the thiol-specific reagent 4,4'-dithiodipyridine (4-PDS) but showed a wide variation in reactivity. Cysteines at positions 317, 318, 320, and 321 showed no reaction with 4-PDS. The mutants on illumination also showed wide variations in activating G<sub>T</sub>. The mutant Y306C showed almost no G<sub>T</sub> activation, I307C and N310C were poor, and the activity of the mutants M309C, F313C, and M317C was also reduced relative to WT. The results suggest that the region comprising amino acids 306–321 is a part of a tertiary structure and that specific amino acids in this region on light-activation participate in the interaction with G<sub>T</sub>.

G-protein-coupled receptors (GPCRs)<sup>1</sup>, the largest known family of cell surface receptors, mediate a wide variety of signal transduction processes. Examples are the sensory systems, vision and smell, neurotransmission, and hormone action. Conformational changes in surface receptor proteins upon the arrival of signals are universally acknowledged as hallmarks in the initiation of signal transduction. A precise molecular description of the tertiary structures involved and the conformational changes in them remains a formidable problem. Ultimately, three-dimensional structures of the receptors at several functional stages are required. However, at this time, such structures are nonexistent for any of the G-protein-coupled receptors. Alternative possibilities are to investigate the structure and function relationships by chemical, biochemical, and biophysical methods. In studies of rhodopsin, one general approach that continues to be used

is the systematic introduction of cysteine residues. The sulfhydryl group in cysteine provides a handle for the attachment of probes for biochemical and biophysical studies.

In previous papers in this series, systematic introduction of single cysteines has been reported in the cytoplasmic regions connecting helices III and IV, and helices V and VI (refs 2–6, Figure 1). In continuing these studies, we now report on single-cysteine replacements one at a time in the sequence 306–321 that extends from the end of helix VII to the palmitoylation sites (Figure 1). An accompanying paper reports on SDSL studies of the structural features and light-dependent changes in these same mutants (7). Two additional accompanying papers report on corresponding studies of the cysteine mutants in the region connecting helices I and II (Figure 1) (8, 11). Another accompanying paper reports on SDSL studies of cysteine mutants introduced in the C-terminal region of rhodopsin (1). Together, the present set of papers completes the systematic introduction of single cysteines at the rhodopsin cytoplasmic face and their studies by SDSL.

The cysteine mutants at positions 306–321 now reported begin near the cytoplasmic end of helix VII and terminate at Cys-322 and Cys-323, the palmitoylation sites. The palmitoyl groups are believed to anchor this region of the cytoplasmic face in the membrane bilayer. The amino acid sequence in this region has been implicated, from peptide competition studies, to be a component in G<sub>T</sub> activation (12). Helix VII carries Lys-296 which is involved in the linkage of 11-*cis*-retinal to rhodopsin through a protonated Schiff base. The latter is involved in interaction with the counterion

<sup>†</sup> This work was supported by NIH Grants GM28289 and NEI EY11716 (H.G.K.) and EY05216 (W.L.H.), the Jules Stein Professorship endowment (W.L.H.), and a grant from the Ford Bundy and Anne Smith Bundy Foundation.

<sup>‡</sup> This is paper 30 in the series "Structure and Function in Rhodopsin". The preceding paper is Langen et al., this issue (ref 1).

<sup>\*</sup> To whom correspondence should be addressed.

<sup>§</sup> Massachusetts Institute of Technology.

<sup>||</sup> Present address: Dept. of Biochemistry, Oregon Health Sciences University, Portland, OR 97201.

<sup>⊥</sup> Present address: Millenium Pharmaceuticals Inc., Cambridge, MA 02139.

<sup>#</sup> University of California.

<sup>1</sup> Abbreviations: DM, dodecyl maltoside; GPCR, G-protein-coupled receptor; Meta II, Metarhodopsin II; 4-PDS, 4,4'-dithiodipyridine; SDSL, site-directed spin labeling; G<sub>T</sub>, transducin; WT, wild type; TM, transmembrane.

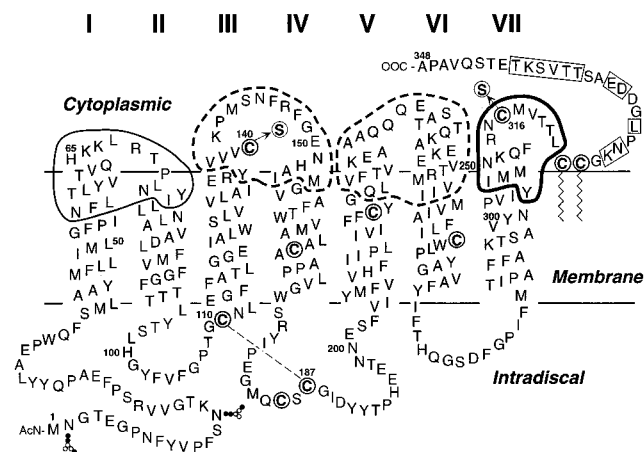


FIGURE 1: A secondary structure model of bovine rhodopsin showing the regions in the cytoplasmic surface where replacements, one at a time, of native amino acids by cysteines have been carried out. The length of each helix and the membrane aqueous boundary were determined by SDSL and electron microscopy studies (3, 5, 7–10). The cysteine mutants described in the present work are within the thick solid line boundary. The cysteine mutations in the cytoplasmic interhelical regions connecting helices III and IV and helices V and VI studied previously (2, 4) are within the dashed line boundaries. The cysteine mutations within the thin solid line boundary and rectangular boxes are described in accompanying papers (1, 8, 11). C140 and C316, the two reactive cysteines in the dark in native rhodopsin, were replaced by serine residues (solid circles), except for the mutant in which the single reactive cysteine was the native C316. Thus, every mutant studied in the cytoplasmic domain contained a single reactive cysteine.

Glu-113 in helix III. Light-catalyzed isomerization of retinal is believed to disrupt this interaction (13). SDSL studies have indicated that a spin label attached at Cys-316 at the top of helix VII (Figure 1) senses a change in its environment upon Meta II formation (14). Moreover, a change in distance between the spin labels at Cys-316 and at Cys-65 accompanies MII formation (15). Perturbation in the environment around helix VII on light-activation has also been demonstrated recently by exposure of an epitope for an antibody specific for the light-activated state of rhodopsin (16).

We report on the properties of the sixteen single-cysteine mutants from Y306C to L321C. Specifically, their chemical reactivity to the sulfhydryl reagent 4-PDS in the dark, the lifetime of the corresponding Meta II species formed on illumination, and the rates of  $G_T$  activation are reported. The results indicate that this region is involved in a tertiary structure, and upon light-activation, specific amino acids in it participate in the interaction with  $G_T$ .

## MATERIALS AND METHODS

11-*cis*-Retinal was a gift from Dr. Rosalie Crouch (University of South Carolina and the National Eye Institute of the National Institutes of Health, U. S. Public Health Services). GTP- $\gamma$ -S was purchased from Boehringer Mannheim (Indianapolis, IN). 4-PDS was purchased from Sigma (St. Louis, MO). DM was from Anatrache (Maumee, OH). Antirhodopsin monoclonal antibody rho-1D4 was purified from myeloma cell lines provided by Dr. R. S. Molday (University of British Columbia) and was coupled to cyanogen bromide-activated Sepharose 4B (Sigma) as described (17). Approximately 10 mg of 1D4 monoclonal antibody was

used for each milliliter of swollen Sepharose beads.  $G_T$  was purified from bovine rod outer segments as described by Baer et al. (18). The nonapeptide corresponding to the C-terminal sequence of rhodopsin, which was used to elute rhodopsin samples from the antibody 1D4-Sepharose matrix, was prepared at the MIT Biopolymers Laboratory.

Buffers used were the following: buffer A, 137 mM NaCl, 2.7 mM KCl, 1.8 mM  $\text{KH}_2\text{PO}_4$ , and 10 mM  $\text{Na}_2\text{HPO}_4$ , pH 7.2; buffer B, buffer A plus 1% (w/vol) DM, 2 mM ATP, 2 mM  $\text{MgCl}_2$ , and 0.1 mM phenylmethylsulfonylfluoride (PMSF); buffer C, buffer A plus 0.05% DM (wt/vol); buffer D, 5 mM 2-(*N*-morpholino)ethanesulfonic acid (MES), pH 6.0, 0.05% DM (wt/vol).

**Construction of Single-Cysteine Mutants in Rhodopsin.** An opsin gene containing the mutations C140S and C316S was constructed previously by Dr. Kevin Ridge (unpublished data). All of the single-cysteine mutants in the sequence 306–321 except mutant C316 were derivatives of this mutant. The mutant containing the single reactive cysteine at position 316 has been previously constructed (19).

Single-cysteine mutants Y306C, I307C, M308C, M309C, N310C, K311C, and Q312C were prepared by fragment replacement mutagenesis in the synthetic gene for bovine opsin (20) as cloned in the expression vector PMT4 (21). The restriction fragments *Pst*I/*Bsp*EI (nucleotides 699–942) containing the single-cysteine substitutions of these constructs were used to replace the *Pst*I/*Bsp*EI fragment of mutant C140S/C316S.

A two-step technique that included PCR mutagenesis was used for preparation of the mutants F313C, R314C, N315C, M317C, V318C, T319C, T320C, and L321C. The first step involved PCR reactions with the C140S/C316S plasmid as the template using the following primers containing the above single-cysteine codon one at a time: the primer 5'-GATGAACAAGCAGTGGCCGGAAGTCT-3' for F313C; the primer 5'-GAACAAGCAGTCTGCAACTCTATG3' for R314C; the primer 5'-GCAGTTCCGGTGTCTATGGTCAC3' for N315C; the primer 5'-CCGGAAGTCTTGGCGTCACTCTCTG3' for M317C; the primer 5'-GGAAGTCTATGTGCACCACTCTCTG3' for V318C; the primer 5'-CTCTATGGTCTGCACTCTCTGCTG3' for T319; the primer 5'-CTCTATGTGCACTCTGCTGCTG3' for T320C; and the primer 5'-GGTCACTCTGCTGCTGTGGCAAG3' for L321C.

The details of the procedure for PCR reaction have been described previously (6). The PCR products were digested to give the corresponding small fragments *Pst*I/*Sal*I (nucleotide 699–1003) containing the single-cysteine substitution sites. These fragments were then subcloned into the vector from the parent plasmid C140S/C316S using the same restriction sites. The DNA sequence of the *Pst*I/*Sal*I fragment containing the mutation site in each construct was confirmed by the dideoxynucleotide sequencing method (22).

**Expression of the Mutant Opsin Genes and Purification of the Expressed Opsin After Reconstitution with 11-*cis*-Retinal.** The procedures for transient transfection of COS-1 cells and treatment of the harvested cells with 11-*cis*-retinal were as described (17). The cells (five 15 cm diameter plates) were harvested 52–56 h post transfection and were solubilized in 5 mL of buffer B for 1 h at 4 °C in the dark. The suspension was then centrifuged for 30 min at 4 °C, and the supernate was mixed with 200  $\mu\text{L}$  of the antibody 1D4-Sepharose beads (approximate binding capacity of 1  $\mu\text{g}$  of

rhodopsin/ $\mu\text{L}$  of resin) for 3 h at 4 °C (17). The resin was washed first with 30 bed volumes (6 mL) of buffer C, followed by a further wash with 15 bed volumes (3 mL) of buffer D. The protein was eluted with buffer D containing 80  $\mu\text{M}$  C-terminal peptide in fractions of 1.5 bed volumes.

**UV/Vis Absorption Spectroscopy.** UV/Vis absorption spectra were recorded using a Perkin-Elmer  $\lambda 7$  spectrophotometer. All spectra were recorded with a bandwidth of 2 nm, a response time of 1 s, and a scan speed of 240 nm/min at 20 °C. The molar extinction value ( $\epsilon_{500}$ ) used for WT rhodopsin was 40 600  $\text{M}^{-1} \text{cm}^{-1}$  (4). For photobleaching, samples were illuminated for 10 s with a 150 W fiber optic light (Fiber Lite A-200; Dolan Jenner, Woburn, MA) equipped with a  $>495$  nm long-pass filter and the spectra were recorded immediately after illumination. Meta II decay rates were measured by the fluorescence assay as described (23).

**Reaction of 4-PDS with Rhodopsin Cysteine Mutants.** The quantitation of protein sulfhydryl groups with 4-PDS has been previously described (6, 24, 25). Mutant samples in buffer D (48  $\mu\text{L}$ ) were mixed with 192  $\mu\text{L}$  of the same buffer containing 4-PDS such that the final solution contained 0.5  $\mu\text{M}$  rhodopsin and 25  $\mu\text{M}$  4-PDS. The reaction at 20 °C was followed by monitoring the absorption of the product 4-thiopyridone at 323 nm with the same concentration of 4-PDS in the reference cuvette. The absorption of rhodopsin alone at this wavelength was subtracted. The molar extinction coefficient of 4-thiopyridone at 323 nm was determined to be 19 000  $\text{M}^{-1} \text{cm}^{-1}$  by titration of L-cysteine with 4-PDS under the same conditions. Due to the large excess of 4-PDS, the reaction is pseudo-first-order in sulfhydryl concentration. Thus, for each reactive mutant, the increase in 4-thiopyridone as a function of time was fitted by a single-exponential function to determine the reaction rate constant.

**$G_T$  Activation Assay.** Activation of  $G_T$  by rhodopsin was monitored using fluorescence spectroscopy (PTI fluorimeter) at 20 °C (4). The excitation wavelength was 295 nm with a 2 nm slit width, and the emission wavelength 340 nm with a 12 nm slit width.  $G_T$  was added to 673  $\mu\text{L}$  of reaction mixture containing 10 mM Tris pH 7.2, 2 mM  $\text{MgCl}_2$ , 100 mM NaCl, 1 mM DTT, and 0.012% DM. The final concentration of  $G_T$  was 250 nM. The solution was stirred for about 300 s to establish a baseline, and photobleached rhodopsin (7  $\mu\text{L}$ ) was added to the mixture to a final concentration of 5 nM. After a further 600 s, GTP- $\gamma$ -S from a stock solution (0.5 mM) was added to the reaction mixture to a final concentration of 5  $\mu\text{M}$ , and the increase of fluorescence was followed for 2000 s. To calculate the relative activation rates, we determined the slopes of the initial fluorescence increase after GTP- $\gamma$ -S addition by linear regression through the data points covering the first 60 s.

## RESULTS

**Characterization of the Single-Cysteine Mutants Y306C–L321C.** In general, the levels of expression in COS-1 cells as judged by the yields of immunoaffinity purified rhodopsin mutants were comparable to WT rhodopsin. All of the purified mutants formed rhodopsin-like chromophore with  $A_{280}/A_{500}$  ratios between 1.6 and 1.8 (Table 1). The absorption  $\lambda_{\text{max}}$  in the visible range varied from 498 to 501 nm. Upon illumination, all mutants formed the characteristic Meta II intermediates. The rate of bleaching for all the mutants was

Table 1: Characterization of Single-Cysteine Substitution Mutants Y306C–L321C

mutant	chromophore $\lambda_{\text{max}}$ (nm)	$A_{280}/A_{500}$ <sup>a</sup>	meta II decay <sup>b</sup> ( $T_{1/2}$ , min)
WT	500	1.6	12.2
Y306C	500	1.7	<b>18.7</b>
I307C	499	1.7	11.6
M308C	499	1.6	11.6
M309C	500	1.6	10.8
N310C	499	1.7	<b>16.9</b>
K311C	500	1.6	10.3
Q312C	499	1.6	12.4
F313C	499	1.8	<b>15.4</b>
R314C	499	1.6	<b>16.1</b>
N315C	499	1.7	11.4
C316	498	1.7	11.2
M317C	498	1.8	10.3
V318C	500	1.7	9.6
T319C	499	1.7	9.8
T320C	499	1.8	12.0
L321C	501	1.8	11.2

<sup>a</sup> The UV/vis absorbance spectral ratios were determined after the elution of rhodopsin from the immunoaffinity matrix at pH 6.0. <sup>b</sup> The  $T_{1/2}$  values for mutants which differ significantly from WT are shown in bold.

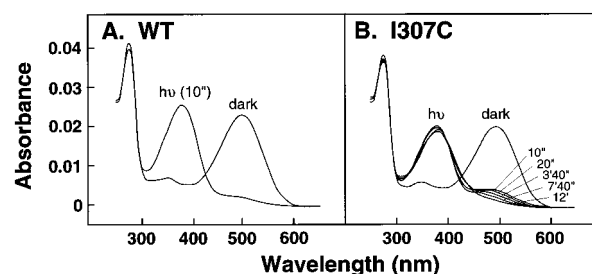


FIGURE 2: UV/Vis spectral properties of WT rhodopsin (A) and mutant I307C (B) in the dark and after light illumination. The abnormal bleaching of mutant I307C is shown by the spectra recorded at different time intervals after illumination.

similar to WT (complete disappearance of the  $\lambda_{500}$  absorption and formation of  $\lambda_{380}$  absorption within 10 s) except for the mutant I307C. This mutant showed abnormal bleaching which was studied further as a function of time. Thus, as seen in Figure 2, absorption at 500 nm of this mutant persisted for up to 12 min of illumination.

The rates of Meta II decay ( $T_{1/2}$ ) after illumination are listed in Table 1. For WT rhodopsin, the  $T_{1/2}$  was 12.2 min under the assay conditions, while the  $T_{1/2}$  for the single-cysteine mutants varied from 9.6 to 18.7 min. Mutants Y306C, N310C, F313C, and R314C showed significant increases in Meta II half-life (bold numbers in Table 1), with Y306C showing the most significant increase.

**Reactivity of the Cysteine Sulfhydryl Groups in Mutants Y306C–L321C to 4-PDS.** The kinetics of reaction of every cysteine mutant with 4-PDS was followed spectrophotometrically by monitoring the absorption at 323 nm as described in “Materials and Methods”. Under the conditions used, WT rhodopsin showed 2 mol of reactive cysteines per mole of rhodopsin (Cys-140 and Cys-316) in the dark (6). The majority of the mutants (M308C–C316 and T319C) incorporated essentially 1 mol of the reagent per mole of the rhodopsin mutant. Reactions with half-lives  $t_{1/2} < 0.5$  min were taken as essentially instantaneous, and such rapid reactions were observed with N310C, Q312C, F313C, and



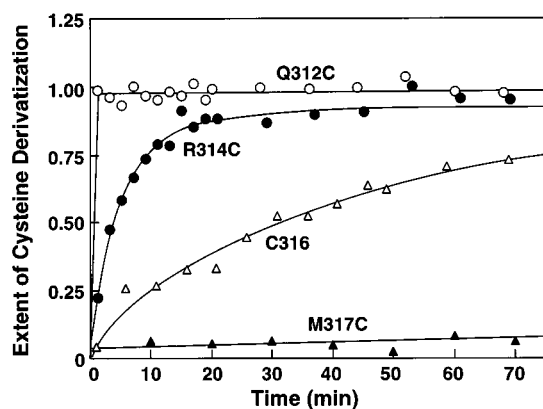


FIGURE 3: Time courses of the reaction of selected single-cysteine mutants with 4-PDS: Q312C (open circles), R314C (solid circles), C316 (open triangles), and M317C (solid triangles). The mutants were immunoaffinity purified at pH 6.0 as described in "Materials and Methods". The derivatization reactions with 4-PDS were carried out at the same pH by monitoring the development of absorbance at  $\lambda_{323}$  due to the 4-thiopyridone formed (Materials and Methods). The extent of derivatization at each time point was calculated using  $19\,000\text{ M}^{-1}\text{ cm}^{-1}$  as the molar extinction coefficient for 4-thiopyridone. Single-exponential fits to the curves are also shown.

Table 2: Comparison of the Reactivity of Cysteine Mutants Y306C–L321C with 4-PDS

mutant <sup>a</sup>	rate ( $\text{min}^{-1}$ ) <sup>b</sup>	mutant <sup>a</sup>	rate ( $\text{min}^{-1}$ ) <sup>b</sup>
Y306C	$0.0020 \pm 0.0005$	Q312C	$>1.4^c$
I307C	$0.0015 \pm 0.0006$	F313C	$>1.4^c$
M308C	$0.062 \pm 0.001$	R314C	$0.18 \pm 0.03$
M309C	$0.018 \pm 0.001$	N315C	$>1.4^c$
N310C	$>1.4^c$	C316	$0.029 \pm 0.001$
K311C	$0.49 \pm 0.04$	T319C	$0.55 \pm 0.11$

<sup>a</sup> No reaction was detected under the conditions used between 4-PDS and the mutants M317C, V318C, T320C, and L321C. <sup>b</sup> Each value of the pseudo-first-order rate constant was the average of at least three measurements. The error given is the standard deviation. <sup>c</sup> These reactions were complete at the first time point taken ( $\sim 0.5$  min).

N315C. While cysteines in mutants K311C and T319C also reacted rapidly with  $t_{1/2} \approx 1.5$  min, mutants M308C, M309C, R314C, and C316 showed slower reaction with 4-PDS with  $t_{1/2}$  in the range from 4.0 to 39 min. Extremely slow reactions were observed with Y306C and I307C ( $t_{1/2} > 300$  min). No detectable reaction was observed with M317C, V318C, T320C, and L321C. Cysteine at position 319 showed surprisingly high reactivity compared with the cysteines in the neighboring positions. The time courses for the reactions and exponential fits for selected mutants are shown in Figure 3, while the pseudo-first-order rate constants for all of the mutants are listed in Table 2.

***G<sub>T</sub> Activation by the Single-Cysteine Mutants.*** Figure 4 shows the rates of fluorescence increase (Materials and Methods) for selected mutants when compared with WT rhodopsin. The initial activation rates for all of the mutants determined by the fluorescence assay are compared in Figure 5. Wide variation in the rates was observed. Some mutants, such as V318C and L321C, showed rates of activation that were similar to that of WT rhodopsin. In contrast, the mutant Y306C showed essentially no  $G_T$  activation, I307C and N310C were poor in activation, and the activity of the mutants M309C, F313C, and M317C was also reduced relative to WT rhodopsin.

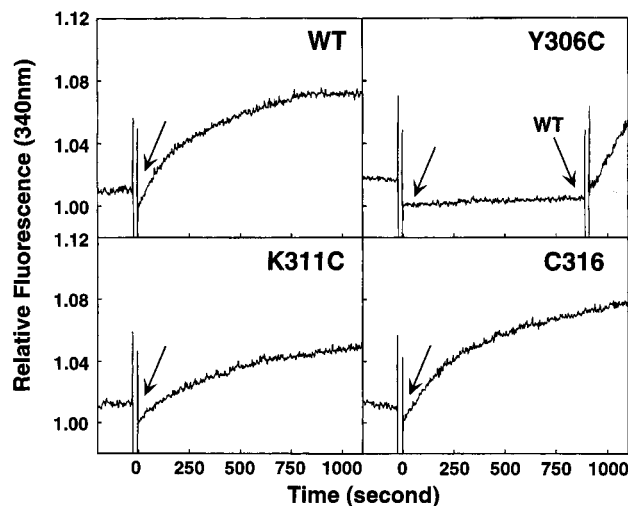


FIGURE 4: Kinetics of  $G_T$  activation by WT rhodopsin and by selected single-cysteine mutants Y306C, K311C, and C316 as determined by the fluorescence increase assay (Materials and Methods). The point of addition of GTP- $\gamma$ -S is indicated by arrows. In the case of the mutant Y306C, which showed no detectable increase in fluorescence, WT rhodopsin was added later, as shown, as an internal control.

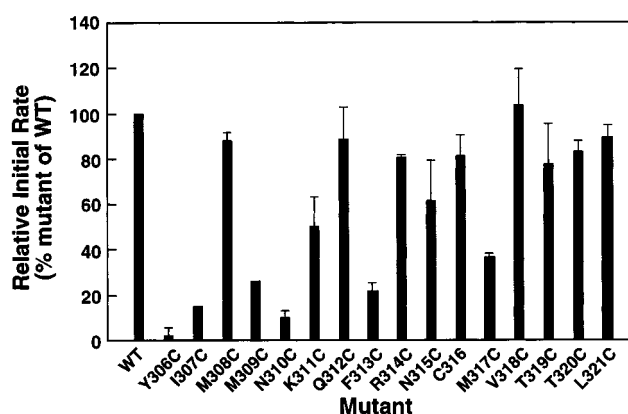


FIGURE 5: Comparison of the relative initial rates for activation of  $G_T$  by the cysteine mutants. Activation of  $G_T$  by each mutant was followed with the fluorescence assay as in Figure 4. The relative initial rates are represented by the rates of fluorescence increase relative to WT. The value for each mutant was determined by linear regression through the data points covering the first minute after GTP- $\gamma$ -S addition. Each value is the average of three measurements.

## DISCUSSION

Structure–function studies on rhodopsin in recent years have all led to the most plausible hypothesis that the three regions, the intradiscal, the TM, and the cytoplasmic region, each have specific tertiary structures in the dark state. Light-catalyzed retinal isomerization causes specific movements in the TM helices resulting in a conformational change in the cytoplasmic domain preparing the molecule for the protein–protein interactions involved in signal transduction (5, 26, 27). Further experimental evidence also strongly indicates that the conformational change in the cytoplasmic face is coupled to structural changes in the TM as well as in the intradiscal region (28). Since the hallmarks in protein functions are their tertiary structures, it must be concluded that the conformational change in the cytoplasmic region involves a change from one tertiary structure to another. The tertiary structure in the cytoplasmic face is presumed to

encompass the four sequences connecting helices I and II, helices III and IV, helices V and VI, and the end of helix VII to the palmitoylated cysteines. The C-terminal tail, from the palmitoylation sites to the C-terminal alanine, does not appear to be a determinant of the tertiary structure in the cytoplasmic domain (1).

A general approach to structural studies of the cytoplasmic face, which involves the systematic introduction of single-cysteine residues along the sequences, has been described in a number of previous publications (2–6). This approach has now been taken to completion in this and the accompanying papers (1, 7, 8, 11). The present paper has reported on studies of the region from the cytoplasmic end of helix VII to the palmitoylated Cys-322 and Cys-323 (Figure 1). This region is of significance from several points of view. Helix VII contains Lys-296, the site of the attachment of 11-*cis*-retinal to the protein by a protonated Schiff base linkage. The latter is uniquely important in spectral tuning and stabilizes the ground-state structure by interaction with the Glu-113 counterion in helix III (13). Further, this region is involved in the interaction with G<sub>T</sub> (12). The adjoining C-terminal region contains multiple phosphorylation sites and is therefore uniquely important in the desensitization process. In addition the carboxyl-terminus is also presumed to be important in intracellular transport of the protein (29, 30). The palmitoylation sites are conserved in all of the visual pigments, and their presence suggests that they anchor this region of the protein to the lipid bilayer. This may explain the nonreactivity of the cysteines at the adjacent positions (317–321) toward 4-PDS.

A number of factors could influence the reactivity of the sulfhydryl groups in different cysteines, including solvent accessibility, disposition within the structure, and the dielectric constant prevailing in the immediate environment. The rates of reaction with 4-PDS are shown in Table 2 for all of the cysteine mutants, while kinetic plots for selected mutants are illustrated in Figure 3. Thus, wide variation in reactivity was observed among cysteines at different positions in the sequence 306–321. One group, which showed no reaction at all using prolonged times under the reaction conditions, is composed of M317C, V318C, T320C, and L321C. In contrast, T319C, sandwiched between the two nonreactive residues, showed high reactivity. Lack of reactivity of a sulfhydryl group in a cysteine implies that the residue is buried either in a tertiary structure or in the hydrophobic micelle interior, where the relatively hydrophilic 4-PDS has low solubility. A second group, comprising N310C, Q312C, F313C, and N315C, reacted so rapidly that their reactions were complete at the first time point taken (about 0.5 min) (see also Figure 3 for Q312C). While Y306C and I307C reacted extremely slowly with 4-PDS, the reactions did reach completion. Cysteines at positions 308, 309, 314, or 316 showed variations, but the rates were intermediate as shown for R314C and C316 in Figure 3. Altogether, among the reactive cysteines, variations in rates of more than 1000-fold were found. Possible relationships between the sulfhydryl reactivity and rhodopsin structure in the various mutants are considered in an accompanying paper (7).

Except for the mutant I307C, all the cysteine mutants formed Meta II normally on illumination (10 s illumination). However, the mutant I307C had abnormal bleaching behavior

as shown in Figure 2. The meaning of this is not clear. The rates of Meta II decay were also normal for the majority of the mutants, except for Y306C, N310C, F313C, and R314C, which showed significantly slower rates of decay (Table 1).

Evidence for the involvement of the amino acid sequence 306–321 in G<sub>T</sub> interaction came from the work of König et al (12). These investigators used synthetic peptides corresponding to specific sequences in rhodopsin to compete with Meta II for binding to G<sub>T</sub>. The results showed that peptides corresponding to the second and third cytoplasmic interhelical sequences, and the sequence from helix VII to the palmitoylation sites (amino acids 310–321), competed effectively with Meta II. Apparently, these sequences are involved in the binding of rhodopsin to G<sub>T</sub>. In the present work, G<sub>T</sub> activation by all the single-cysteine mutants through the sequence 306–321 was studied. The effects of the point mutations on G<sub>T</sub> activation after illumination varied widely. Thus, mutants Y306C, I307C, M309C, N310C, F313C, and M317C all showed a striking decrease in activity, while Y306C did not activate G<sub>T</sub> at all (Figure 4 and Figure 5). Our results not only confirm the previous findings on the involvement of sequence 310–321 in the G<sub>T</sub> interaction (12) but also identify individual amino acids in the region 306–321 that are critical for the interaction.

There are two possible explanations for the inhibitory effect of specific point mutations on G<sub>T</sub> activation. One possibility is that the substituted native amino acid is one of the critical residues presented to and directly recognized by G<sub>T</sub> after light illumination. Replacement of such a residue with cysteine could affect the interaction of rhodopsin with G<sub>T</sub>. Indeed, a synthetic peptide without the interaction with other regions in native rhodopsin is unlikely to form a specific tertiary structure alone that could be recognized by G<sub>T</sub>. In this case the ability of the peptide (310–321) to bind G<sub>T</sub> as observed by König et al. (12) could arise from the initial interaction of G<sub>T</sub> with specific residues in the peptide, followed by a change to the correct conformation of the peptide. The second possibility is that the effects of the cysteine mutations on G<sub>T</sub> activation are due to structural perturbations in the photoactivated state of rhodopsin. At this stage, it is not possible to distinguish between the above two possibilities for the reduced activation of G<sub>T</sub> by the mutants Y306C, I307C, M309C, N310C, F313C, and M317C.

Of further interest is the observation that mutant Y306C, while it showed a longer Meta II half-life than that of WT, did not activate G<sub>T</sub>. In this mutant, the cysteine substitution occurred in the sequence NP(X)<sub>n</sub>Y, a highly conserved motif in the GPCR family. This sequence has been postulated to play a role in the agonist-induced internalization of the receptors. Recently, it has been shown that the mutation of Y to A in  $\alpha_{1B}$ -adrenergic receptor increased the affinity for agonist by 10-fold, but it abolished G-protein activation (31). Our findings with the mutant Y306C appear to be similar to the above observations in regard to lack of G<sub>T</sub> activation and the prolonged Meta II half-life, which could be due to a higher affinity for the agonist, all-trans retinal.

## ACKNOWLEDGMENT

We thank Professor U. L. RajBhandary of MIT Biology Department and members of this laboratory for the helpful

discussions. Ms. Judy Carlin's assistance during the manuscript preparation is gratefully acknowledged.

## REFERENCES

1. Langen, R., Cai, K., Altenbach, C., Khorana, H. G., and Hubbell, W. L. (1999) *Biochemistry* 38, 7918–7924.
2. Ridge, K. D., Zhang, C., and Khorana, H. G. (1995) *Biochemistry* 34, 8804–8811.
3. Farahbakhsh, Z. T., Ridge, K. D., Khorana, H. G., and Hubbell, W. L. (1995) *Biochemistry* 34, 8812–8819.
4. Yang, K., Farrens, D. L., Hubbell, W. L., and Khorana, H. G. (1996) *Biochemistry* 35, 12464–12469.
5. Altenbach, C., Yang, K., Farrens, D. L., Farahbakhsh, Z. T., Khorana, H. G., and Hubbell, W. L. (1996) *Biochemistry* 35, 12470–12478.
6. Cai, K., Langen, R., Hubbell, W. L., and Khorana, H. G. (1997) *Proc. Natl. Acad. Sci. U.S.A.* 94, 14267–14272.
7. Altenbach, C., Cai, K., Khorana, H. G., and Hubbell, W. L. (1999) *Biochemistry* 38, 7931–7937.
8. Altenbach, C., Klein-Seetharaman, J., Khorana, H. G., and Hubbell, W. L. (1999) *Biochemistry* 38, 7945–7949.
9. Unger, U. M., Hargrave, P. A., Baldwin, J. M., and Schertler, G. F. X. (1997) *Nature* 389, 203–206.
10. Baldwin, J. M., Schertler, G. F. X., and Unger, U. M. (1997) *J. Mol. Biol.* 272, 144–164.
11. Klein-Seetharaman, J., Hwa, J., Cai, K., Altenbach, C., Hubbell, W. L., and Khorana, H. G. (1999) *Biochemistry* 38, 7938–7944.
12. Konig, B., Arendt, A., McDowell, J. H., Kahlert, M., Hargrave, P. A., and Hofmann, K. P. (1989) *Proc. Natl. Acad. Sci. U.S.A.* 86, 6878–6882.
13. Sakmar, T. P., Franke, R. R., and Khorana, H. G. (1989) *Proc. Natl. Acad. Sci. U.S.A.* 86, 8309–8313.
14. Resek, J. F., Farahbakhsh, Z. T., Hubbell, W. L., and Khorana, H. G. (1993) *Biochemistry* 32, 12025–12031.
15. Yang, K., Farrens, D. L., Altenbach, C., Farahbakhsh, Z. T., Hubbell, W. L., and Khorana, H. G. (1996) *Biochemistry* 35, 14040–14046.
16. Abdulaev, N. G., and Ridge, K. D. (1998) *Proc. Natl. Acad. Sci. U.S.A.* 95, 12854–12859.
17. Oprian, D. D., Molday, R. S., Kaufman, R. J., and Khorana, H. G. (1987) *Proc. Natl. Acad. Sci. U.S.A.* 84, 8874–8878.
18. Baehr, W., Morita, E. A., Swanson, R. J., and Applebury, M. L. (1982) *J. Biol. Chem.* 257, 6452–6460.
19. Resek, J. R., Farrens, D. L., and Khorana, H. G. (1994) *Proc. Natl. Acad. Sci. U.S.A.* 91, 7643–7647.
20. Ferretti, L., Karnik, S. S., Khorana, H. G., Nassal, M., and Oprian, D. D. (1986) *Proc. Natl. Acad. Sci. U.S.A.* 83, 599–603.
21. Franke, R. R., Sakmar, T. P., Oprian, D. D., and Khorana, H. G. (1988) *J. Biol. Chem.* 263, 2119–2122.
22. Sanger, F., Nicklen, S., and Coulson, A. R. (1977) *Proc. Natl. Acad. Sci. U.S.A.* 74, 5463–5467.
23. Farrens, D. L., and Khorana, H. G. (1995) *J. Biol. Chem.* 270, 5073–5076.
24. Grassetti, D. R., and Murray, J. F., Jr. (1967) *Arch. Biochem. Biophys.* 119, 41–49.
25. Chen, Y. S., and Hubbell, W. L. (1978) *Membr. Biochem. I*, 107–129.
26. Farrens, D. L., Altenbach, C., Yang, K., Hubbell, W. L., and Khorana, H. G. (1996) *Science* 274, 768–770.
27. Farahbakhsh, Z., Hideg, K., and Hubbell, W. (1993) *Science* 262, 1416–1420.
28. Ridge, K. D., Lu, Z., Liu, X., and Khorana, H. G. (1995) *Biochemistry* 34, 3261–3267.
29. Deretic, D., Puleo-Schepke, B., and Tripp, C. (1996) *J. Biol. Chem.* 271, 2276–2286.
30. Deretic, D., Schmerl, S., Hargrave, P. A., Arendt, A., and McDowell, J. H. (1998) *Proc. Natl. Acad. Sci. U.S.A.* 95, 10620–10625.
31. Wang, J., Zheng, J., Anderson, J. L., and Toews, M. L. (1997) *Mol. Pharmacol.* 52, 306–313.

BI9900119